A Comparison of Elastic Moduli Derived from Theory, Microindentation, and Ultrasonic Testing

Susan K. Lum[1] and Wendy C. Duncan-Hewitt[2,3]

Received May 13, 1996; accepted August 20, 1996

Purpose. The objective of our work was to evaluate the elastic modulus through ultrasonic testing of poly(methyl methacrylate-co-methacrylic acid) (PMMA/coMAA), a viscoelastic polymer similar to the commercial Eudragit®, to calculate this modulus, assuming a regular arrangement of interacting groups, and ultimately, assess the accuracy of microindentation as a means of evaluating elasticity in very small samples.

Methods. Knoop indentation testing was performed on cast samples using a Tukon testing apparatus. Solid density and pulse echo testing employing a damped 15 MHz transducer served to quantify the elastic moduli. Using the Hoy method of calculation for molar attraction constants, and assuming pairwise addition, the modulus was calculated and compared with typical experimental values for amorphous and crystalline polymers.

Results. Acoustic testing resulted in an average elastic modulus value of 5.67 ± 0.2 GPa for this copolymer, which concurs with literature values for PMMA. Acoustically derived experimental moduli when normalized and plotted against calculated values, resulted in a relationship, $E/(1 - 2\upsilon) = 17.0\ (E_{coh} + x_c\Delta Hm)/V + 6.9$, similar to that predicted in theory.

Conclusions. Indentation contact modeling does not adequately describe the real recovery under indentation. In contrast, acoustic testing of pharmaceutical materials affords a simple, reproducible means of characterizing moduli without impairing structural integrity. Acoustically derived moduli further afford insight into the intermolecular interactions, as expressed by the interaction energy terms.

KEY WORDS: microindentation; ultrasonic testing; elastic modulus.

[1] Faculty of Pharmacy, University of Toronto, 19 Russell Street, Toronto, Ontario Canada M5S 2S2.

[2] Assistant Dean, School of Pharmacy, Texas Tech, Amarillo, Texas 79106.

[3] To whom correspondence should be addressed.

ABBREVIATIONS: ρ, density (g/mL); α, a constant; ΔH_m, the heat of fusion (kJ/mol); Δt, the time difference between signal peaks (s); A_H, the Hamaker constant in a vacuum (J); C, the atom-atom pair potential coefficient (J · m^6); E, elastic modulus (MPa); ε_1, dielectric constant; E_{coh}, the molar cohesive energy (J/mol); E_{subl}, the lattice or sublimation energy of the molecular crystal (J/mol); F, molar attraction function ($J^{1/2} \cdot cm^{3/2}$/mol); G, shear modulus (MPa); *h*, sample thickness (m); h, Planck's constant; H_k, hardness number (MPa); k, Boltzmann's constant; K, bulk modulus (MPa); L, length of the long axis of the indentation (mm); n_1, the refractive index; p, pressure (MPa); P, load (N); u_L, longitudinal wave velocity (m/s); u_S, the shear wave velocity (m/s); V, molar volume (cm^3/mol); *v*, the Poisson's ratio; v_e, the absorption frequency (Hz); W, short axis dimension under indentation (mm); W′, the relaxed short axis dimension when the indenter is removed (mm); x_c, the degree of crystallinity (a fraction of 1).

INTRODUCTION

The elastic properties of solids reflect their resistance to tension, (Young's modulus E), to compression (bulk modulus K) and to shear and are due to the strength of the interatomic or intermolecular forces. The elastic modulus of a material is then an intrinsic measure of the overall strength of a solid. In solid-state pharmaceutics, elastic modulus information may be of value specifically, because elasticity plays an important role in compaction and probably is a major contributor to the capping phenomenon.

There are many methods available to assess the elasticity of engineering materials. Many pharmaceutical solids, however, are normally available only as finely divided powders which are mechanically and chemically labile. For these materials, one often is faced with making a choice among methodologies, none of which is entirely satisfactory (1).

For example, microindentation techniques allow direct testing of microscopic, single crystals. The primary limitation of indentation testing for determining modulus values is that the micromechanics of the material below the indenter and the complex contact geometry are not well understood and the results are, therefore, difficult to interpret. Microindentation does not provide a direct measure of elastic modulus, rather, it has been used as an empirical predictor for the modulus, given the hardness of a material (2). Allowing for the complex contact configuration in indentation, only approximate solutions for deformation under an indenter are available for even elastic-plastic contact (3). Calibration factors are required to compare indentation-derived modulus results with those determined by other experimental methods (1). Microindentation, then, permits the evaluation of single crystal properties, but it in itself is reliant upon a model of indentation response.

Alternatively, sound has long been used for testing materials. Ultrasonic assessment of true material elastic constants, however, requires fully dense specimens without the presence of internal stresses such as those generated during compaction. Single crystal assessment is complicated by anisotropy, the need to cut specimens of appropriate geometry and edge effects when the specimens are small. Single crystals of appropriate size often are difficult to grow. These problems are not present in relatively isotropic materials, such as unoriented polymers which can be formed fully dense by non-mechanical means.

Ultrasound or high frequency (0.1 to 25 MHz) vibrations are propagated by means of waves; internal defects are detected by the change in the propagated sound. Acoustic testing can be used to inspect a sample for internal stresses, flaws, strength and toughness, without impairing its functional integrity (4). Changes in ultrasonic spectra, interpreted as microstructural changes, provides information about material microstructure and morphology (5).

Sound propagation has been used to evaluate the particle size in suspensions (6) and the porosity of powder compacts (7, 8, 9). The theory underlying the reflection, propagation, absorption and scattering by materials and flaws is well documented (5).

In tablets, pores are examples of detectable flaws. Ketolainen et al. (1995) (8) used laser-generated ultrasound to describe changes in tablet modulus with porosity. The exponential relation between signal intensity and porosity could then

0724-8741/96/1100-1739$09.50/0

be back extrapolated to zero porosity to obtain the modulus of the tablet's constituent material. The physical constraints of ultrasonic equipment limits the application of ultrasound to large samples or compacts; precluding most single crystal testing.

Macroscopic engineering tests such as the three- or four-point beam, Chevron notch, and double torsion test, require large fully dense specimens of defined geometries that are difficult to produce for most pharmaceutical materials.

The research described in this paper was undertaken to explore the error arising from the use of different methods in order to assist in making appropriate choices in the assessment of the elasticity of pharmaceutical materials.

BACKGROUND

Indentation and Elastic Recovery

The elastic moduli of materials have been found frequently through a force-displacement relationship during microindentation with a concomitant depth sensing device or through scanning electron microscopic measurements of indentations (1, 10). In circumstances where such equipment is unavailable, however, other techniques must be employed.

In testing of our copolymer material, we resorted to the determination of the ratio of hardness to elastic modulus (H/E) through indentation with a Knoop pyramid indenter, using a model which has successfully predicted the modulus of various ceramics and metals (1), using loads producing indents devoid of fracture flaws. Upon unloading there is some elastic recovery related to H/E, in the depth of the indent. The apparent hardness number (H_k) is derived from the projected area of the indentation using:

$$H_k = 14.2 \times P \times L^{-2} \tag{1}$$

where P is the load and L is the length of the long indentation diagonal. Upon unloading, the displacement due to elastic recovery beneath the plastic zone may be calculated by assuming the indentation is analogous to a simple elliptical indentation. Superposition of the solutions (11) for a two-dimensional elliptical hole subject to an uniaxial stress provides an estimate of this displacement due to relaxation of elastic strain:

$$W - W' = (\alpha L p)/E \tag{2}$$

In equation 2, W is the short axis dimension under load, W' is the relaxed dimension when the indenter is removed, L is the long axis of the indentation, p is the pressure and α is a constant. Very little recovery of the length of the long diagonal of the indentation occurs after the load is removed (12).

By substituting the pressure p with H_k and noting that W/L is close to 1/7.11 for Knoop geometry, equation 2 reduces to

$$\frac{W'}{L} = \frac{W}{L} - \alpha \frac{H_k}{E} \tag{3}$$

A calibration curve for a series of materials of known hardness and elastic modulus provides a value for α (~0.45) (2). Thus

$$E = \frac{0.45 H_k}{\frac{1}{7.11} - \frac{W'}{L}} \tag{4}$$

has been used to provide elastic moduli of materials.

Elasticity and Sonic Velocity in Solids

When ultrasonic energy waves of a certain frequency propagate through a material, its constituent molecules are vibrated at that frequency, resulting in a displacement from equilibrium intermolecular positions. The rate at which this vibration propagates through the material, or the specific wave velocity for the medium, is dependent on both the material inertia and the material elasticity. The elastic constant for the material is related to this wave velocity, the velocity of sound in solids, through (13)

$$u_L^2 = \frac{K}{\rho} \times \frac{3(1 - \nu)}{(1 + \nu)} \tag{5}$$

where u_L is the ultrasound (longitudinal wave) velocity in the material, K the bulk modulus and ρ is the density of the material.

E and K are linked by the standard elasticity relation:

$$E = 3K(1 - 2\nu) \tag{6}$$

Anisotropic solids would require characterization of the elastic parameters as a function of the crystallographic direction. For such solids, not only would the longitudinal wave velocity u_L, in which particles vibrate in the same direction as the motion of sound be required, but also the shear wave velocity component u_s, in which particles vibrate in a direction that is orthogonal to the motion of sound.

Ultrasound Generation

One method used to produce ultrasonic vibrations in a solid is to employ a transmitter that applies high frequency electrical pulses to a piezoelectric transducer. When energized with electrical pulses the piezoelectric transducer transforms the electrical energy into mechanical sound vibrations and transmits these vibrations through a coupling medium, such as oil or water (which serves as the acoustic link), into the test material. Two transducers may be used for ultrasound transmission and reception (pitch-catch method) or both functions may be performed by one transducer (pulse-echo method). This configuration is useful for objects accessible only from one side (5).

Ultrasonic readings can also be used as a test of homogeneity. The transmitted beam continues through a sample until it meets an acoustic-impedance mismatch (a crack, inclusion or back wall) whereupon some of the wave energy is reflected to the transducer, producing an 'echo' pulse on screen. A discontinuity would prevent the transmission of the beam to the back wall and would reflect less of the incident energy in a shorter time of travel. The time lapse would be proportional to the distance of the discontinuity from the entering surface (14).

Correlation of Moduli with Chemical Structure

The elastic modulus originates from the dependence of the energy of interaction between molecules and their distance of separation. Empirical relationships between this elastic parameter and other physical properties have included the Gruneisen-Tobolsky relation (15) for simple molecular crystals which is given by

$$K = 8.04 \times \frac{E_{subl}}{V} \tag{7}$$

$$E_{subl} \approx E_{coh} + x_c \Delta H_m \tag{8}$$

Thus combining equations 6, 7, and 8 provides

$$\frac{E}{(1 - 2\nu)} \approx 24.1\left(\frac{E_{coh}}{V} + \frac{x_c \Delta H_m}{V}\right) \tag{9}$$

where ΔH_m is the heat of fusion (kJ/mol), x_c the degree of crystallinity, V the molar volume, E_{coh} the molar cohesive energy, and E_{subl} the lattice or sublimation energy of the molecular crystal. Similar work has been reported by Roberts et. al. (1991) (16) for crystalline powders wherein a relation between the solubility parameters and the Young's modulus was also based on the Tobolsky relation. The solubility parameter concept, however, is strictly applicable only to amorphous polymers (13, 15). Highly crystalline polymers such as polyethylene and poly(tetrafluoroethylene) (PTFE) are insoluble in all solvents at room temperature, while they obey solubility parameters rules at $T > 0.9\ T_m$. The adaptation of the cohesive energy density concept to semi-crystalline and crystalline polymers must then explicitly address the heat of fusion (ΔH_m) in the free enthalpy balance relation (13).

In this paper the concept of cohesive interactions in relation to the Young's modulus for polymers has been extended to include the influence of crystallinity through an explicit ΔH_m term.

MATERIALS AND METHODS

Specimen Preparation

Polymethylmethacrylate/comethacrylic acid (PMMA/coMAA) an amorphous acrylic polymer similar to the commercial pharmaceutical Eudragit® was chosen for study. Although the flow and materials behavior of polymethylmethacrylate (PMMA) alone is well documented, the copolymer is more commonly employed in pharmaceutical coating and encapsulation processes, is markedly softer, can be directly compressed and exhibits minimal fracture under compressive loading.

PMMA/coMAA cylinders were prepared by free radical bulk polymerization of a mixture of (50:50 wt%) of inhibitor-free methyl methacrylate (MMA) and inhibitor-free methacrylic acid (MAA) using recrystallized azo-isobutyrlnitrate (AIBN) as the initiator. The mixture was degassed through repeated freeze-thawing under an argon blanket and the polymerization carried out in sealed glass molds under argon at 25°C for 4 weeks. The resulting cylinders were purified by extracting any residual monomer, side products, or initiator in a soxhlet reflux. Slab matrices of thickness 4.73 to 5.05 mm were prepared by microtoming after swelling in MeOH/water (60/40 by volume). The samples for this study were annealed at 120°C for 2 hours prior to further testing.

These samples when tested using differential scanning calorimetry (DSC)(Perkin-Elmer 2C) at 10 degrees/min from 0 to 300°C, displayed no peaks associated with the presence of crystallites.

The material density, determined by a pycnometer method using helium as an inert gas, was modestly temperature dependent and equal to 1.25 g/mL − (0.002) × temp(°C) SE = ±0.001 g/mL (Quantachrome Stereo pycnometer model SPV-2 #171, courtesy of Ortho-McNeil).

Microhardness Testing

The Knoop hardness was found using a Tukon Miniload microindentation hardness tester (Model 300) equipped with a Knoop diamond pyramid indenter and microscope unit. The indenter was cleaned with acetone and allowed to dry. It was then lowered slowly onto the surface of the sample by a hydraulic mechanism over a period of 15 s and the full load was maintained for 10 s. The indenter was then raised automatically. Indentations were measured using the scale in the eyepiece of the microscope which was calibrated daily. The mean diameter of five indentations per sample was used to calculate the Knoop hardness values and the corresponding elastic moduli.

Immersion Testing

An immersion pulse-echo configuration was used. The pulse-echo system consisted essentially of an oscillator providing alternating current bursts, a sending/receiving piezoelectric transducer, a signal amplifier, a cathode ray tube for display, as well as the necessary power supply. When an impinging signal strikes the surface, part is reflected to the transducer and the rest transmitted. The time elapsed between the transmission of the pulse and the return of the echo from the back wall of the sample is a measure of the speed of the traveling wave through the specimen. The separation of the successive echoes from the front and back surfaces of a sample requires the layer thickness to be greater than half of the length of the ultrasonic pulse.

The first wave reflected at the backwall transmits only a small portion of its energy to the probe when it arrives at the front wall. Thereafter attenuated by the material and reflected from the front wall, it propagates through the specimen a second time, and so forth. Any one of the echo signals may be isolated for detailed study by a process known as gating. An effective gating was achieved by using the 'delay' on an oscilloscope to isolate the signal of interest.

Scans were produced using a Panametrics 5055PR (Panametrics, Waltham, MA) pulser-receiver (courtesy of Dr. A. Sinclair, Mechanical Engineering, *U* of *T*). The damping control, which varies the shunt resistance across the transducer, was set for maximum damping. Transducers ranging from 10 MHz to 30 MHz were tested to determine the optimum frequency for testing. A moderately damped 15 MHz 12.7 mm diameter transducer (Panametrics V313 15/0.25 #68733) was used. The range of the target from the transducer was approximately 3 cm. The target specimen consisted of a slab of acrylic copolymer (PMMA/MAA) which was carefully aligned perpendicular to the transducer to obtain the maximum specular echo. Each specimen was measured in triplicate for thickness by a micrometer and the time for wave travel recorded. This time and thickness were then converted to a longitudinal wave velocity for that sample:

$$u_L = \frac{2h}{\Delta t} \tag{10}$$

where h is the sample thickness and Δt the time difference between signal peaks. The reflected echo signal from a single

interface as downloaded from the analog oscilloscope is shown in Figure 1.

Immersion in water links the transducer acoustically to the test specimen and overcomes the difficulty of ensuring good vibration coupling to a medium. The copolymer employed was insoluble in water. There were losses in the vibration energy, as evidenced by the continuous decrease in reflected signals; the amplitude of the propagated echoes diminished with time. This copolymer is viscoelastic which tends to highly attenuate the sonic echoes (5). In addition to the attenuation of the material, this decrease was also caused by the energy loss of the wave due to the coupled probe when reflected at its contact surface, and secondly by the divergence of the sound beam.

Calculation of Moduli by Additive Group Contributions

For a number of amorphous and semi-crystalline polymers, the energy of cohesion was determined from tables of group molar attraction constants using the method of Hoy (13) which was preferred over other methods in predicting the cohesive energy with a mean accuracy of about 10%. The technique is illustrated in Figure 2 for the 1:1 random bulk polymerized copolymer PMMA/coMAA.

Alternatively, in colloid and surface chemistry, intermolecular and interparticle forces are often quoted in terms of the Hamaker constant A_H, with a usual range of 4 to 40 $\times$ 10^{-20} J. Lifshitz theory affords the derivation of A_H in terms of macroscopic bulk properties such as the dielectric constant and refractive index. This approach overcomes the 'many-body' problem of interacting dipoles. It side-steps the atomic or particulate structure view of the solid and treats the solid instead as a continuous medium. (For an informative discussion see Israelachvili (17)) Thus

$$A_H = \frac{3}{4} kT\left(\frac{\varepsilon_1 - 1}{\varepsilon_1 + 1}\right)^2 + \frac{3h\nu_e(n_1^2 - 1)^2}{16\sqrt{2}(n_1^2 + 1)^{3/2}} \quad (11)$$

$$C = A_H V^2/\pi^2 \quad (12)$$

where A_H is the Hamaker constant in a vacuum, C the atom-atom pair potential coefficient, ε_1 dielectric constant, n_1 the refractive index, ν_e the absorption frequency.

By assuming a regular arrangement of particles, the bulk modulus relating the variation of the internal energy of an assembly of monomer units with separation, has been calculated as (18)

$$K = \frac{14.4C}{V^3} \quad (13)$$

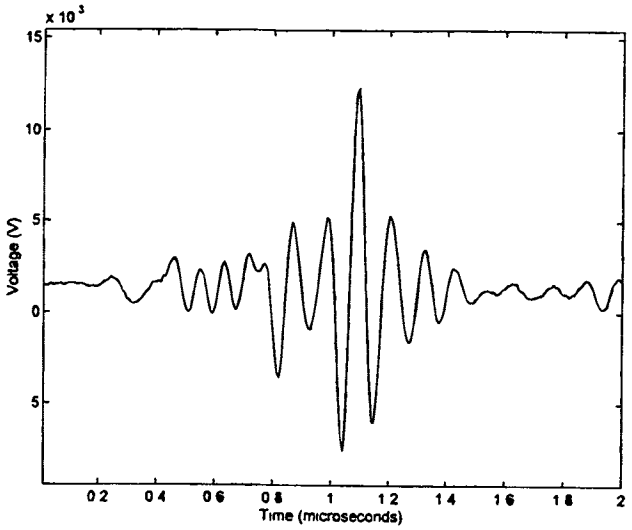

Fig. 1. Echo signal of the PMMA/coMAA slab specimen measured using a damped transducer with a frequency band of 15MHz, as displayed on an analog oscilloscope.

RESULTS

The Knoop hardness values of the polymer matrices which averaged 11.3 $\pm$ 3.9 MPa, are summarized in Table I. The elastic moduli based on Equation 4 are also tabulated.

The results of sonic velocity measurements, performed on samples of thickness 4.73–5.05 mm are tabulated in Table II. The average acoustic velocity for the PMMA/coMAA samples were between 2.6 to 2.8 $\times$ 10^3 m/s. It was found that at the relatively high frequency, 15 MHz range, viscoelastic flow is inhibited, and therefore the apparent modulus approaches 5.8 GPa. The apparent modulus drops to about 5.1 GPa at low frequency (10 MHz).

To compare theoretical and experimentally derived values, the measured normalized Young's moduli (Table IIIa) were plotted against the theoretically determined moduli (using Equation 9 and Table IIIb) in Figure 3. The values of ΔH_m for the crystalline polymers (polystyrene (PS), PTFE, and methylcellulose) were tabulated from the literature (13) and used in equation (9) for calculation as shown in Table IIIb. Literature data was used in preference in the calculations for microcrystalline methyl-cellulose, as the monomer unit favored induced dipole moments.

Calculations of moduli based upon bulk properties, A_H, are presented in Table IV.

DISCUSSION

Changes in material morphology and properties among sample matrices were monitored through microhardness testing. As shown in Table I, microhardness test results vary quite widely with a standard deviation on the order of 35%. As alluded to earlier, the indentation contact configuration is complex and exact solutions describing this contact do not exist. Simplifications were adopted in order to derive the elastic modulus; the indent was modeled as a two-dimensional elliptical hole (2) under uniaxial stress. However, the simplified picture of the indentation field falls short of describing the actual elastic zones involved. The problem can be linked to the following considerations: First of all, the strain-rate resulting from the indentation geometry of loading is inversely time dependent. This complicates the measurements in viscoelastic samples as the material response is rate dependent; the time between indentation, recovery, and measurement would need to be standardized. Secondly, the stress field below the indenter is non-uniform. The simplifying assumptions adopted in the description of the contact zone evolution would need to be modified to describe the actual zones involved.

The elastic modulus values ranging from -3.43×10^2 to $+2.03 \times 10^2$ MPa as predicted by this model are not feasible. The negative values associated with the moduli are an obvious

Polymethacrylic acid (PMAA) Polymethylmethacrylate (PMMA)

$$F^2 = E_{coh} \times V$$

PMAA	functional group	F contribution	PMMA	functional group	F contribution
	base	277.0		base	277.0
	$-CH_3$	303.4		$-(CH_3)_2$	606.8
	$-CH_2-$	269.0		$-CH_2-$	269.0
	>CH-	176.0		>CH-	176.0
	-COOH	1000.1		-COO-	668.2
	Σ	2025.5		Σ	1997.2
	∴Ecoh (J/mol)	5.83×10^4		∴Ecoh (J/mol)	4.66×10^4
	∴1:1 random	copolymer	average	Ecoh (J/mol)	$= 5.24\times10^4$

Fig. 2. Calculation of the molar attraction constant, *F*, and the energy of cohesion of 1:1 PMMA/coMAA using group contribution terms as per the method of Hoy[13].

indication that the assumptions used simply do not apply in this context. Our measured *W'/L* ratio fell below the ideal *W/L* ratio of 1/7.11 for Knoop geometry which rendered a negative *E* value. This arbitrarily assumed ratio (1:7.11) is based on the indenter angle geometry for an isotropic, ideal plastic material which produces an indent with length:depth:breadth of 30.53:1:4.29. For real viscoelastic/plastic materials, this ratio may be expected to fall below this value.

The response of our copolymer material to applied stress fields is extremely time sensitive and as such, the variable time lag in performing the indentation (10 s) and examining the resultant deformation would contribute greatly to the variation observed. A better measure of the initial unrecovered *W/L* ratio would involve direct measurement (ie. through adapted atomic force microscopy) over a restricted time scale.

Furthermore, the gradient α value was adjusted to fit a series of materials with known *E* and H_k. This calibration curve may not be valid for the material tested; another curve encompassing the expected value of the modulus would need to be constructed. For these reasons, modulus determination through

Table I. Microhardness Testing Using a Knoop Indenter. Hardness Values Average 11.3 ± 3.9 MPa

Sample No.	Long Diagonal *L* (μm)	Short Diagonal *W* (μm)	Hardness H_k (MPa)	Elastic Modulus *E* (MPa)
1	3.916×10^2	4.517×10^1	9.092×10^0	1.62×10^2
2	2.967×10^2	8.000×10^1	1.584×10^1	-5.52×10^1
3	2.777×10^2	4.580×10^1	1.809×10^1	-3.43×10^2
4	3.376×10^2	3.420×10^1	1.223×10^1	1.40×10^2
5	4.388×10^2	4.560×10^1	7.241×10^0	8.88×10^1
6	3.038×10^2	5.000×10^1	1.511×10^1	-2.83×10^2
7	4.668×10^2	5.900×10^1	6.400×10^0	2.03×10^2
8	4.074×10^2	4.470×10^1	8.402×10^0	1.22×10^2
9	3.133×10^2	1.806×10^1	1.420×10^1	7.71×10^1
10	4.079×10^2	4.463×10^1	8.381×10^0	1.21×10^2
11	3.808×10^2	1.853×10^1	9.618×10^0	4.71×10^1

Table II. Ultrasonic Determination of Elastic Modulus of PMMA/coMAA Matrices. Average Elastic Modulus Was Found to Be 5.67 ± 0.2 GPa

Sample No.	Thickness (mm)	Acoustic Velocity $\times10^3$ (m/s)	Elastic Modulus (GPa)
1	5.224 (±0.003)	2.587 (±0.017)	5.44 (±0.07)
2	5.295 (±0.006)	2.580 (±0.032)	5.40 (±0.13)
3	4.841 (±0.007)	2.772 (±0.035)	6.24 (±0.16)
4	5.047 (±0.003)	2.656 (±0.033)	5.73 (±0.14)
5	4.160 (±0.021)	2.649 (±0.028)	5.70 (±0.12)
6	4.296 (±0.012)	2.660 (±0.033)	5.49 (±0.30)
7	5.570 (±0.029)	2.537 (±0.029)	5.23 (±0.12)
8	4.572 (±0.010)	2.660 (±0.029)	5.74 (±0.13)
9	4.808 (±0.004)	2.637 (±0.032)	5.64 (±0.10)
10	5.562 (±0.006)	2.684 (±0.057)	5.85 (±0.25)
11	4.222 (±0.015)	2.685 (±0.039)	5.85 (±0.17)

Table IIIa. Elastic Modulus of Various Pharmaceutical Polymers as Obtained from Longitudinal Propagated Ultrasonic Velocity

Sample	Molar Volume (V) (cm^3/mol)	Poisson's Ratio (υ)	Acoustic Velocity (u_L) $\times 10^3$ (m/s)	Elastic Modulus (E) (GPa)
Methylcellulose	214.2[21]	0.30[21]	—	7.09[21]
PMMA	85.6[19]	0.34[19]	2690[19]	5.50
PMMA/ coMMA	74.6[19]	0.34	2646	5.67
Polypropylene	46.3[19]	0.34[19]	2650[19]	4.15
Polystyrene	99.1[19]	0.35[19]	2400[19]	3.77
PTFE	45.9[19]	0.31[19]	1380[19]	2.99
PVC	45.0[20]	0.35[20]	2180[20]	4.12

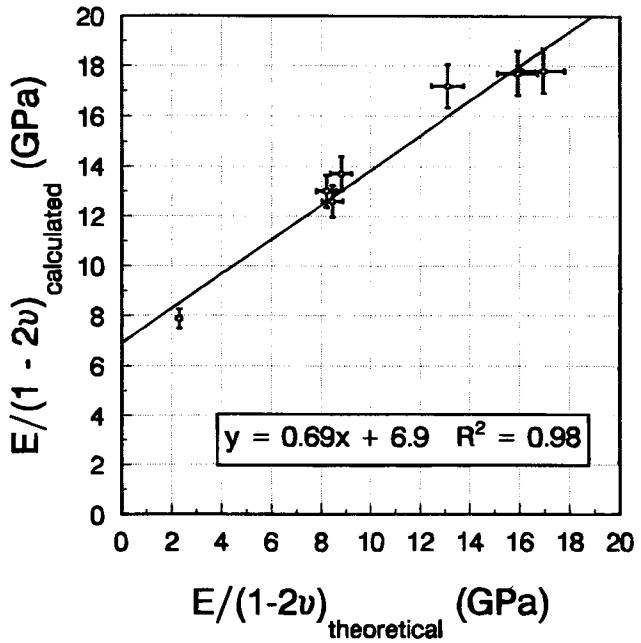

Fig. 3. Normalized elastic moduli calculated from experimental data vs. normalized moduli determined theoretically.

Knoop indentation testing alone is not preferred in the context of polymeric materials testing. It may still suffice for fully crystalline materials such as sucrose as demonstrated by Duncan-Hewitt (1988) (23). To make the Knoop test more generally useful, it might be necessary to evaluate unique calibration factors for different families (23) of materials (eg. FCC metals, organic crystals, polymers).

Acoustic testing in contrast provides reproducible values for the elastic modulus (see Table II). The microsecond timescale associated with ultrasonic measurements was conducive in decreasing this variability. The measured average acoustic velocity for the copolymer cited above is in accordance with the documented values for most polymers (between 2 to 3 mm/microsecond or km/s) (5). Moreover, the average values for E, 5.67 ± 0.4 GPa, of PMMA/coMMA lie within the range of Young's modulus values for engineering polymers delineated in Ashby's (1992) materials properties charts (24).

Several damped frequency transducers (10MHz to 30MHz) were used to determine the optimum frequency for testing; the elastic modulus of a viscoelastic material is dependent on the rate or time period of loading. A time delay exists in the strain response of a viscoelastic material to applied stress. The variable loading used in pulse-echo testing then results in a strain response which varies in a similar sinusoidal manner as the applied stress, but it is out of phase.

Increasing the frequency of the pulse-transducer usually increases resolution in ultrasonic testing, however, the nature of a viscoelastic material as described above tends to 'damp' the applied stress. This occurs at the natural frequency for main chain rotation in the polymer structure and is particularly strong at the glass transition. On the molecular level, when high frequencies are applied, there is insufficient time for chain uncoiling to occur and the material will exhibit relative stiffness. In contrast, when lower frequencies are applied, the chains have relatively more time to move in response, and the polymer will appear relatively rubbery. It is not unexpected, then, that the copolymer exhibits an apparently higher modulus at 15MHz and an apparently lower modulus at 10MHz. At even higher frequencies, the material attenuates the signal to the extent that the peak associated with material interaction is indistinguishable from baseline noise.

The pulse echo method is reproducible but simple and uses only a pulse-transducer for triggering and receiving signals. Unfortunately, acoustic linking for the sample and the transducer are required. Immersion in water or other media must be used judiciously, since many pharmaceutical materials will be soluble in them. In contrast, pulsed laser generation methods as used by Ketolainen et al. (1995) (8), although equipment intensive, are more likely to preserve the intrinsic structural integrity of the material. Samples would require coupling to the testing apparatus through taping to one side alone. Back calculation to zero porosity for powdered compacts provides the values necessary to calculate moduli of powdered materials (8).

Table IIIb. Theoretical Moduli Calculated from Cohesive Energy Corrected for the Influence of Crystallinity

Sample	Cohesive Energy (E_{coh}) (J/mol)	Crystallinity Ratio (x_c)	$(E_{coh} + x_c \Delta H_m)/V$ (MPa)	Elastic Modulus (E) (GPa)
Methylcellulose	1.41×10^5 [21]	0.7[21]	660.6	6.37
PMMA	4.66×10^4 [13]	0.0[13]	544.3	4.20
PMMA/coMMA	5.24×10^4 [13]	0.0	702.8	5.42
Polypropylene	1.58×10^4 [13]	0.5[13]	340.2	2.63
Polystyrene	3.47×10^4 [13]	0.0[13]	350.1	2.60
PTFE	4.40×10^3 [13]	1.0[13]	95.86	0.88
PVC	1.65×10^4 [13]	0.0[13]	365.0	2.64

Table IV. Theoretical Moduli Calculated in Terms of Macroscopic Bulk Properties[17,22]

Sample	Dielectric Constant (ε_1)	Refractive Index (n_1)	Absorption Freq. (Hz)	Hamaker Constant (A_H) (J)	Elastic Modulus (E) (GPa)
PMMA	2.87	1.492	2.9×10^{15}	1.15×10^{-19}	2.26
PTFE	2.10	1.359	2.9×10^{15}	3.84×10^{-20}	1.68
PVC	3.20	1.527	5.0×10^{15}	7.52×10^{-20}	2.64

It can be seen in Figure 3, that there is good agreement between the theoretically calculated and the experimentally determined moduli. The deviation in the predicted relationship may be attributed to a number of factors including the possibility of induced dipole moments and hydrogen bonds which cannot be accounted for through additive group contributions. Ultrasonic measurements were measured through longitudinal velocities alone. The accuracy in the modulus values may be improved through concomitant measurement of shear velocities.

The relation with cohesive energy differs from that reported by Roberts et al. (1991) (16) for various crystalline powders. This was not unexpected as the heat of fusion term was explicitly incorporated in our treatment in order to extend the theory beyond that for amorphous polymers alone. Moreover, the experimentally derived moduli used by Roberts et al. (16) was based upon three point beam testing. Such testing required recasting of the pharmaceutical powders and such macroscopic static tests would be affected by flaws in the cast specimen.

Using bulk properties, in Table IV, we see that the calculated modulus for these amorphous polymers are somewhat smaller than the observed values but agree to within a factor of 2. The derivations of equations (11 to 13) assume a regular, rigid structure, whereas polymeric subunits are in continuous thermal motion and are somewhat disordered. A better agreement would not be expected.

CONCLUSIONS

Pharmaceutical materials present an unique challenge to the assessment of elasticity. Microindentation approaches, although applicable in samples as small as 100 μm in diameter, require calibration with macroscopic tests and appropriate calibration factors are not available for many types of materials. Macroscopic tests must be performed on compacts and so are subject to inaccuracies resulting from the presence of internal stresses, flaws, and the need to extrapolate to zero porosity to evaluate "true material" parameters. Ultrasonic testing requires smaller specimens than many engineering tests, but these still must be of the order of 1 cm in size to avoid complications due to edge effects. The need for acoustic coupling is also a limitation when one wishes to test soluble materials. Mathematical approaches are limited by the theories and approximations upon which they are based. Given all these considerations, it is probably desirable to use, and compare the results, of several methods while keeping in mind the type and magnitude of error expected in each.

ACKNOWLEDGMENTS

The authors gratefully acknowledge the support provided by the National Sciences and Engineering Council (grant to W. D. H.) and by the Medical Research Council of Canada for this work in the form of a grant to W. D. H and a studentship (to S. L.).

REFERENCES

1. I. J. McColm. *Ceramic Hardness*, Plenum Press, New York, 1990.
2. D. B. Marshall, T. Noma, and A. G. Evans. *Comm. Amer. Cer. Soc.* **65**:C175–C177 (1982).
3. K. L. Johnson. *Contact Mechanics*, Cambridge University Press, Cambridge, 1985.
4. A. Vary. *Materials Evaluation* **51**(3):380–387 (1993).
5. J. Krautkramer and H. Krautkramer. *Ultrasonic Testing of Materials*, 3rd edition, Springer-Verlag, New York, 1983.
6. H. K. Kytomaa. *Powd. Tech.* **82**:115–121 (1995).
7. A. K. Maitra and K. K. Phani. *J. Mater. Sci.* **29**:4415–4419 (1994).
8. J. Ketolainen, M. Oksanen, J. Rantala, J. Stor-Pellinen, M. Luukkala, and P. Paronen. *Int. J. Pharm.* **125**:45–53 (1995).
9. K. K. Phani, S. K. Niyogi, and A. K. Maitra et al. *J. Mater. Sci.* **21**:4335–4341 (1986).
10. B. Rother. *J. Mater. Sci.* **30**:5394–5398 (1995).
11. S. P. Timoshenko and J. N. Goodier. *Theory of Elasticity*, 2nd ed., McGraw-Hill, New York, 1951.
12. D. Tabor. *The Hardness of Metals*, Clarendon Press, Oxford, 1951.
13. D. W. Van Krevelen, (ed.), *Properties of Polymers: their correlation with chemical structure: their numerical estimation and prediction from additive contributions*, 3rd ed., Elsevier, Amsterdam, 1990. pp. 876.
14. W. E. Schalle. *Non-Destructive Testing*, Machinery Publishing Co. Ltd., Brighton, 1968.
15. A. V. Tobolsky. *Properties and Structure of Polymers*, John Wiley & Sons, Inc., New York, 1960. p. 12, 75.
16. R. J. Roberts, R. C. Rowe, and P. York. *Powder Tech.* **65**:139–146 (1991).
17. J. N. Israelachvili. *Intermolecular and Surface Forces*, 2nd. ed., Academic Press, London, 1992.
18. D. Tabor. *Polymer* **35**(13):2759–2763 (1994).
19. B. Hartmann. Acoustic Properties in *Encyclopedia of Polymer Science and Engineering*; 2nd ed., vol. 1, Wiley, New York, 1984. pp. 131–160.
20. A. A. Higazy, M. E. Kassem, A. Y. Kandeil, and R. R. Zahran. *Materials Letters* **20**:237–244 (1994).
21. R. J. Roberts and R. C. Rowe. *Int. J. Pharm.* **99**:157–164 (1993).
22. W. Wunderlich. *The Polymer Handbook*, Bandrupt, P. (ed.), (1975):V55–V57.
23. W. C. Duncan-Hewitt. *The Use of Microindentation Techniques to Assess the Ability of Pharmaceutical Crystals to Form Strong Compacts* Ph.D. Dissertation, University of Toronto, 1988.
24. M. F. Ashby. *Materials Selection in Mechanical Design: Materials and Process Selection Charts*, Pergamon Press, Oxford, 1992.